Bull. Mater. Sci., Vol. 34, No. 4, July 2011, pp. 793–798. © Indian Academy of Sciences.

Interface-dependent resistance switching in $Nd_{0.7}Sr_{0.3}MnO_3$ ceramics

S S CHEN, C P YANG[1,*], C L REN, R L WANG, H WANG, I V MEDVEDEVA[2] and K BAERNER[3]

Faculty of Physics and Electronic Technology, Hubei University, Wuhan 430062, P.R. China
[1]State Key Laboratory of Metastable Materials Science and Technology, Yanshan University, Qinhuangdao 066004, China
[2]Institute of Metal Physics, Ural Division of the Russian Academy of Sciences, Ekaterinburg 620041, Russia
[3]Department of Physics, University of Göttingen, Tammanstrasse 1-37077 Göttingen, Germany

MS received 31 March 2010; revised 10 May 2010

Abstract. **Interface-dependent electric-pulse-induced resistance switching effect (EPIR) in $Nd_{0.7}Sr_{0.3}MnO_3$ ceramics was studied. The results reveal that the EPIR effect originates from the interface between the electrodes and the bulk, and the EPIR ratio as well as the high and low resistance states can be strongly influenced by applying a large electrical field on the sample for different intervals. Also, the pulse parameters have great effect on the stability of EPIR and the optimal pulse width, pulse amplitude and read bias are obtained. Based on the space charge limited current mechanism together with the theory of interfacial charge-trapped state, the interface-dependent resistance switching effect is discussed.**

Keywords. **EPIR; interface; space charge limited current; manganite; resistance-switching.**

1. Introduction

Alkali-earth doped perovskite-type manganites $R_{1-x}A_xMnO_3$ (R = rare-earth and A = alkali-earth) have been studied extensively due to their various unique properties, such as an insulator-metal transition accompanying a ferromagnetic transition (Urushibara *et al* 1995), field-induced structural change (Asamitsu *et al* 1996), colossal magnetoresistance effect (CMR) (Chahara *et al* 1993) as well as the counterpart of CMR, colossal electroresistance effect (CER) (Gao and Hu 2005). Most recently, the electric-pulse-induced-resistance (EPIR) switching effect, which is based on the CER effect, has been discovered and has attracted considerable interest due to its possible applications in memory elements (Liu *et al* 2000). The EPIR effect manifests that the value of resistance can jump between different resistance states if being stimulated by electric pulses with different polarity and amplitude. The unique transport property has an enormous potential for resistance random access memory (ReRAM) due to its nonvolatility, low power consumption, small bit cell size as well as fast switching speed. Despite of the increasing volume of researches in this field, the physical mechanism of EPIR is still not clear, in particular, whether the resistance switching originates from the intrinsic bulk or from the extrinsic interface between the electrodes and the surface of oxide. Different models are available to understand the reversible switching effect, including models as a Schottky barrier with trapped charge state at the interface (Blom 1994), space-charge-limited current (SCLC) (Hickmott 1962), phonon-assisted tunneling (Contreras 2003), formation and rupture of filaments in bulk (Sharpe and Palmer 1996), and redox effect at the interface region (Waser *et al* 2009). However, the EPIR effect can be understood only partially or qualitatively based on the above mentioned models and is far beyond a general model to understand the mysterious transport behaviour.

In earlier studies, the EPIR effect is only observed in thin films of manganites with intrinsic electronic phase separation, i.e. the coexistence of a charge ordered (CO) insulating phase and a ferromagnetic metallic phase, such as in the typical composition of $La_{0.67}Ca_{0.33}MnO_3$ (Sun *et al* 2005) and $Pr_{0.7}Ca_{0.3}MnO_3$ (Peng *et al* 2006). In this work, we report an obvious EPIR effect in the $Nd_{0.7}Sr_{0.3}MnO_3$ ceramic without the intrinsic electronic phase separation, and the results reveal that, besides the pulse parameters, the electric field also has a great effect on the resistance switching effect and the high/low resistance.

2. Experimental

Polycrystalline $Nd_{0.7}Sr_{0.3}MnO_3$ with perovskite structure was prepared using the conventional solid-state reaction

*Author for correspondence (cpyang@hubu.edu.cn)

method. High-purity powders of Nd_2O_3, $SrCO_3$ and MnO_2 were used as raw materials. Nd_2O_3, $SrCO_3$ were pre-treated at 1173 K for 6 h and 673 K for 4 h, respectively before being mixed for eliminating moisture. Powder X-ray diffraction (DRON-3, Cu-K_α, Japan) and scanning electron microscopy (coupled EDS) were utilized to identify the phase purity and to determine the composition of the sample, respectively. Bar electrodes with 1·5 mm width and 4·0 mm length were fabricated on a surface of sample using Ag-paint, and the spacing of each electrode was about 1·2 mm. In order to investigate the effect of different electrode materials on EPIR, copper, aluminium and magnesium electrodes with almost the same geometry as Ag-glue were also deposited on the ceramic surface. Especially, silvering electrode which can form an ohmic contact with the bulk was also prepared by sintering the electrode at 853 K for 20 min in air. The resistance switching effect was investigated between these electrodes using a 2-wire measuring mode. All the data were collected using a Keithley 2400 multimeter with a computer controlled program at room temperature.

3. Results and discussion

3.1 *The interface and bulk resistance*

Besides the alternating current (a.c.) impedance spectra, the bulk resistance and the interfacial resistance can also be separated using different resistance measuring modes, such as the 2-wire and 4-wire schemes shown in the inset of figure 1. For comparison, the 2-wire and 4-wire R using Ag-glue electrode under room temperature are given in the main panel of figure 1. One can see that the 2-wire R between 2 Ag-glue electrodes is about 15·5 ohm and keeps almost the same value, while $R <$ 0·3 ohm is obtained for the 4-wire scheme though measured under the same mode of constant current with 50 μA as the 2-wire. Clearly, the 4-wire R is only the bulk resistance, and it eliminates the lead wire together with the interfacial contact contributions. For the 2-wire scheme the resistance includes not only bulk resistance, but also the interfacial contact resistance, even though it also excludes the lead wire resistance (see the upper left insets in figure 1). The 2-wire R is about two orders of magnitude larger than that of 4-wire, giving us a clue that the 4-wire R is negligible and the interfacial properties may dominate the electrical transport under the 2-wire R measurement mode.

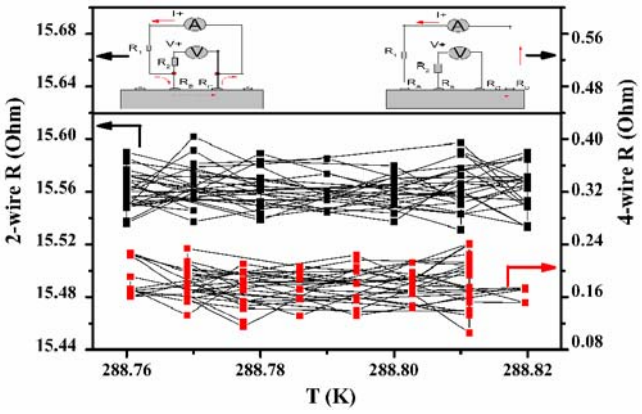

Figure 1. A comparison of the 4-wire R and the 2-wire R for the present sample. The upper insets show the schematic pictures of experimental setup for 2-wire and 4-wire R measurements, respectively.

3.2 *The effect of pulse parameters on the stability of EPIR effect*

The EPIR effect is clearly observed for the Ag-glue electrode after applying a pulse on the sample under 2-wire scheme and the effect of various pulse parameters on EPIR effect are as shown in figures 2 and 3. The high resistance (R_H) and low resistance (R_L) were detected using a small read bias of 0·01 V at room temperature to be 17 and 13·5 ohm, respectively after applying pulses with width (t_0) of 100 μS and pulses amplitude (A) of 5 V on the sample. Clearly, from figure 2(a), the EPIR ratio (here, we define the EPIR ratio as $(R_H - R_L)/R_L \times 100\%$) is 26%. Both the R_H and R_L are much closer to the 2-wire R than the 4-wire R, which implies that the EPIR effect is related to the interface between the electrode and the bulk but not to the bulk only, this is consistent with that reported previously by us (Chen *et al* 2010), where the bulk does not show the EPIR effect via investigating the 4-wire R. Additionally, from figure 2, it is seen that it becomes unstable gradually by increasing the pulse width from 100 μS to 2 S (see figures 2b–d), suggesting that smaller pulse width is advantageous to the stability of EPIR and in present case the optimal width is about 100 μS. Furthermore, the effect of optimal pulse amplitude and read bias on the EPIR effect are also investigated, and shown in figures 3a–f. The optimal pulse amplitude and read bias are respectively 5 V and 0·01 V. Besides, the temperature also has an effect on the EPIR ratio, the details have been described in our previous publication (Chen *et al* 2010).

For investigating the effect of electrode materials on the EPIR effect, copper, aluminium and magnesium electrodes are deposited on the surface of ceramic, and we also measure the EPIR effect under 2-wire measuring mode. The results are similar to that of Ag-glue electrode. However, it is quite different if we adopt the silvering electrode which can form an ohmic contact with the bulk due to the Ag particles diffusing into the bulk deeply during the process of preparing silvering electrodes. This suggests that the EPIR effect in the present case is interface-dependent. The properties of different material electrodes on EPIR are summarized in table 1.

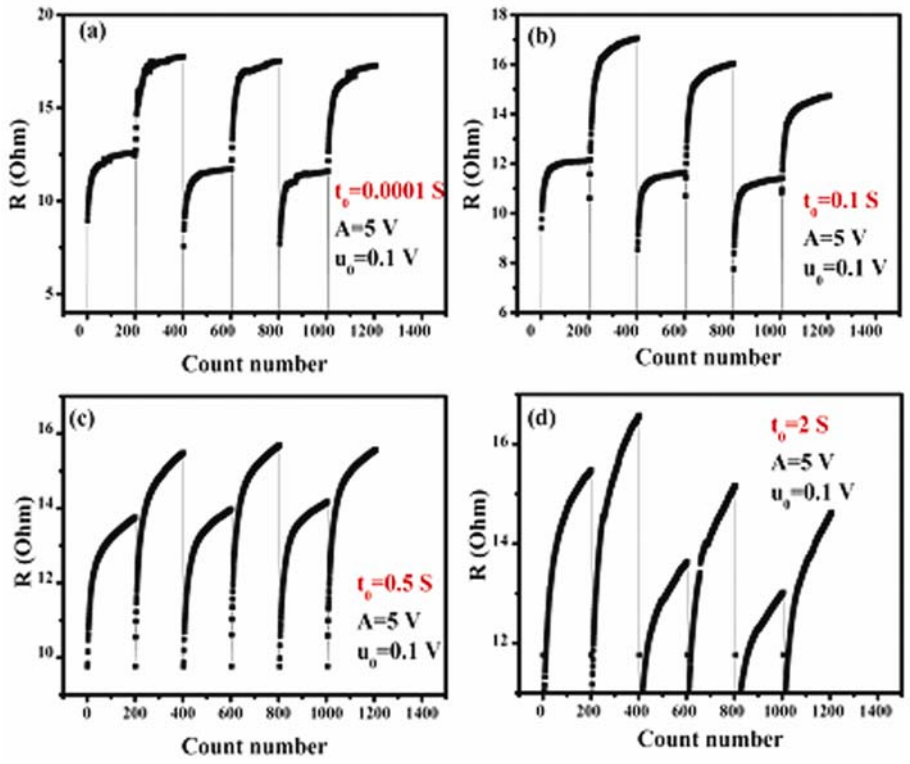

Figure 2. The effect of pulse width on the stability of EPIR.

Table 1. The effect of different electrode materials on the EPIR.

Characteristics		Electrode materials				
		Copper	Aluminium	Magnesium	Ag-glue	Silvering
I–V	Hysteresis	Yes	Yes	Yes	Yes	No
	Rectifying	Yes	Yes	Yes	Yes	No
EPIR		Yes	Yes	Yes	Yes	No

3.3 *The effect of electrical field on interfacial transport*

Except for the pulse parameters and electrode materials, the external electric field can also influence the EPIR effect, as shown in figure 4. Typically, the EPIR effect is obtained using the optimal pulse parameters under 2 wire Ag-glue measuring mode. A direct current (DC) of 1 A is used to examine the effect of electric field on the interfacial transport. Interestingly, the EPIR ratio decreases and even disappears by injecting the direct current for different intervals, for example, the R_H and R_L are turned into 7·2 ohm and 6·8 ohm, respectively from initial values of 17 and 13·5 ohm after injecting current with 1A for 20 s (figure 4b), and continue to drop to almost the same value of 1·8 ohm after continuing to inject current for another 20 s (figure 4c) and to a lower value of 1·4 ohm after about 10 min, accompanied by the disappearance of EPIR effect and a slight climb in resistance (figure 4d). The gradual increase of resistance may result from the joule heat produced in the interface.

The variation of interfacial transport can also be reflected from the $I(V)$ curves shown in figure 5. At the initial state (figure 5a), a remarkable nonlinear $I(V)$ curve is observed. However, the resistance decreases gradually with prolonging the time of injecting current and goes down to a stable value. Meanwhile, the nonlinear $I(V)$ characteristic disappears, being replaced by ohmic behaviour. This is consistent with the data from figure 4.

3.4 *Discussion on the interfacial transport behaviour*

For further understanding the interface-dependent transport, we measure the $I(V)$ curve through two Ag-glue electrodes and plot as a double-logarithmic in the positive bias branch. The scanning rate is 0·1 V/s. The I–V patterns are slightly different from that reflected in figure 5a due to the different bias ranges. As shown in figure 6, at low bias regions of less than 0·1 V, the slope of Ln(I) is

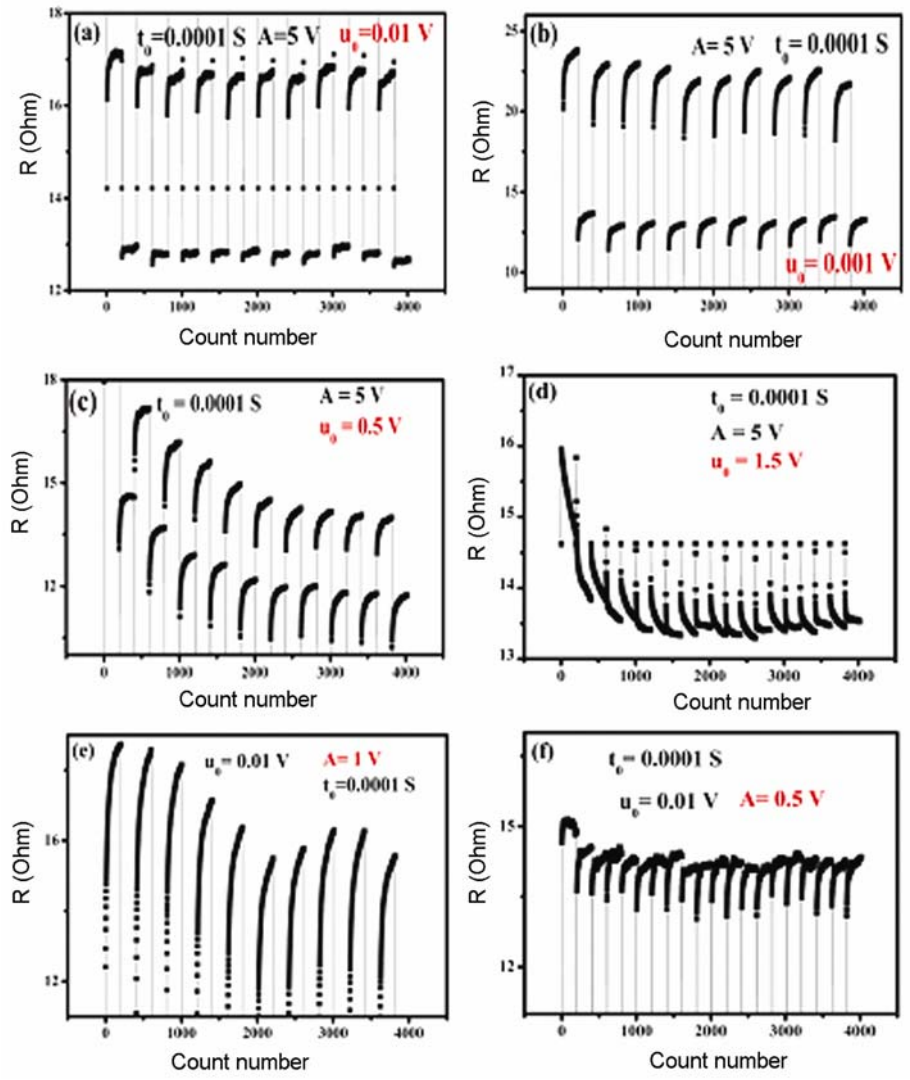

Figure 3. The effect of pulse amplitude and read bias on the stability of EPIR.

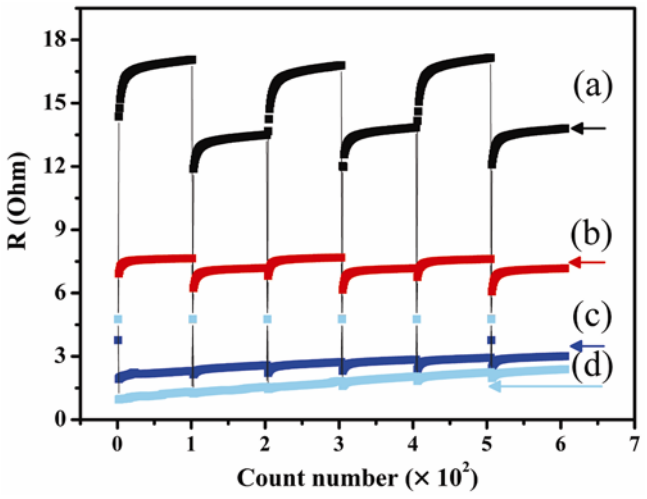

Figure 4. The R_H and R_L versus count number for 2-wire Ag-glue electrodes when injecting 1 A current at different intervals: (a) 0 s, (b) 20 s, (c) 40 s and (d) 10 min.

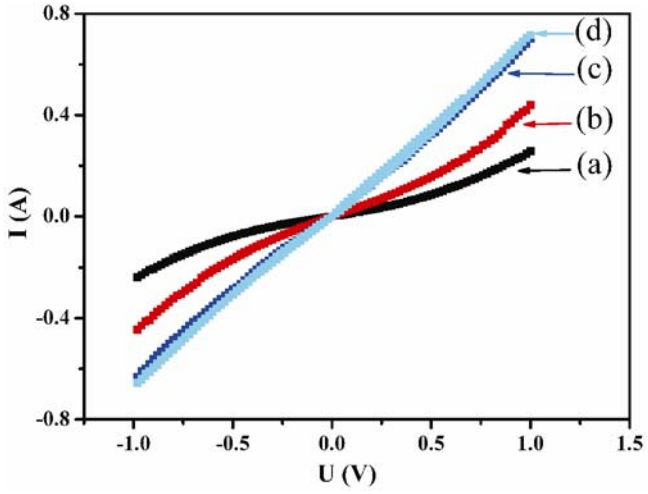

Figure 5. The *I–V* curve of sample scanned from –1 V to 1 V with a rate of 0·1 V/s after being injected 1 A current for different intervals: (a) 0 s, (b) 20 s, (c) 40 s and (d) 10 min.

close to 1, which corresponds to an ohmic transport behaviour. In this bias range, free carriers generated thermally inside the sample would be predominant over the injected charge carriers thus leading to the validity of Ohm's law. At higher bias regions, for example above 0·4 V, the double-logarithm plot demonstrates a change in the slope, which goes up to 1·73, that is in agreement with the space-charge-limited current (SCLC) and trapped-charge-limited current (TCLC) modes. Within the voltages ranging from 0·4 V–1·3 V, charge carriers trapped by the trap-centres located at the interface are de-trapping gradually and the $I(V)$ curve follows the shallow charge trap mode. This is consistent with that reported by Xie *et al* (2006). At higher bias voltage, however, the TCLC mode is realized because all the charge carriers trapped are de-trapping. In the investigated sample, the charge carrier's de-trapping limited voltage (V_{TFL}) is about 1·31 V. Above 1·31 V, the conduction is hardly influenced by these defects and dramatically increases with bias voltages, as a result, the curve slope goes up to 6·08. On bias voltage decreasing from 2 V to 0, the carrier transport transforms directly into SCLC with single shallow trap mode and then follows Ohm's law with a slope of 1·02. In our case, the interfacial transport follows the SCLC/TCLC even though it is a bulky conduction effect; this is consistent with the work of Boer de and Morpurgo (2005), in which the I–V characteristics show bulklike feature of SCLC conduction on the condition that surface traps dominate the transport. Accordingly, we attribute the SCLC/TCLC conduction in Ag/NSMO/Ag heterostructures to the interface induced bulk-like limited transport behaviour.

In the present case, one may also note that the stable interfacial resistance, is much larger than that of the bulk resistance (see figure 1). Considering the metal/semiconductor contact, the Schottky barrier may be formed at Ag/NdSrMnO interfaces due to different work function values of Ag (4·3 eV) and NdSrMnO (4·92 eV) (Reagor *et al* 2004). However, the $I(V)$ curves show a linear behaviour within 0·1 V (inset of figure 6), indicating that the Schottky barrier is not the determining factor for the appearance of large interfacial resistance. The large resistance may result from a resistive region due to the oxygen diffusion from the NdSr–manganite into the Ag electrodes, which results in an oxygen depleted NdSrMnO interfacial layer. At this depleted interface region, various defects such as impurity, oxygen vacancies, A-site vacancies, and Mn^{4+} interstitials as well as dislocations may exist and act as the trapping centres to regulate the interfacial transport and EPIR effect. When intense electric field is applied on the sample, in fact, at the interface, charge carriers trapped by trap-centres are de-trapped rapidly and the interfacial transport is mainly governed by the intense external field as reflected in figures 4 and 5. Moreover, in this polystalline NdSr–manganite, the contribution of grain boundary on the EPIR effect will be small, since a very small contribution (< 0·3 ohm) and a conductive grain boundary are present for stoichiometric NdSr–manganite (Yang *et al* 2007).

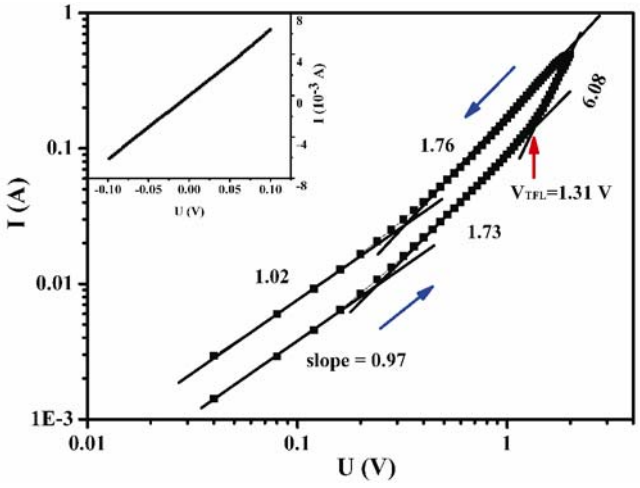

Figure 6. $I(V)$ characteristics of the present sample in a double-logarithmic plot. Arrows indicate the bias voltages scanning direction. The inset shows the linear and symmetrical I–V property when bias voltage sweeps from –0·1 V to 0·1 V.

4. Conclusions

In summary, the resistance switching effect of strontium doped $Nd_{0.7}Sr_{0.3}MnO_3$ ceramic has been investigated. The results show that various pulse parameters can greatly influence the stability of EPIR effect. Experimentally, in our case the optimal pulse parameters are respectively 100 μS, 5 V and 0·01 V. Except for the pulse parameters, a large d.c. electrical field can also strongly affect the interfacial transport and EPIR effect as well as the R_H and R_L, which clearly shows that the EPIR effect originates from the interface between electrode and the bulk. The study on electric transport with different electrode materials also supports this conclusion. Based on models of SCLC and the trapped states located at the interface, the possible EPIR mechanism and unique interfacial transport are discussed. Additionally, the investigation is helpful for both fundamental study and application in devices based on CER manganites.

Acknowledgement

This work is supported by the Natural Science Foundation of China (Grant No. 11074067 and 10911120055/A0402), the Program of the Ministry of Education of P.R. China (New Century Excellent Talents in University, No. NCET-08-0674), and the joint Chinese-Russian Project (Grant No. 08-02-92205).

References

Asamitsu A *et al* 1996 *Phys. Rev.* **B54** 1716
Boer de R W I and Morpurgo A F 2005 *Phys. Rev.* **B72** 073207
Blom P W M 1994 *Phys. Rev. Lett.* **73** 2107
Chahara K I *et al* 1993 *Appl. Phys. Lett.* **63** 1990
Chen S S *et al* 2010 *Solid State Commun.* **150** 240
Contreras J R 2003 *Appl. Phys. Lett.* **83** 4595
Gao J and Hu F X 2005 *Appl. Phys. Lett.* **86** 92504
Hickmott T W 1962 *J. Appl. Phys.* **33** 2669
Liu S Q *et al* 2000 *Appl. Phys. Lett.* **76** 2749
Peng W C *et al* 2006 *J. Appl. Phys.* **100** 093704
Reagor D W *et al* 2004 *J. Appl. Phys.* **95** 7971
Sharpe R G and Palmer P W 1996 *J. Appl. Phys.* **79** 8565
Sun J R *et al* 2005 *Appl. Phys. Lett.* **86** 242507
Urushibara A *et al* 1995 *Phys. Rev.* **B51** 14103
Waser R *et al* 2009 *Adv. Mater.* **21** 2632
Xie Y W *et al* 2006 *J. Appl. Phys.* **100** 033704
Yang C P *et al* 2007 *Acta Phys. Sin.* **56** 4908